

Impact of the Future Climate and Land Use Changes on the Hydrology and Water Resources in South East England, UK

Afzal M., R. Ragab*

UK Centre for Ecology & Hydrology (UK CEH), Wallingford, Oxfordshire, OX10 8BB, UK

*Corresponding author: rag@ceh.ac.uk

Received August 26, 2020; Revised September 28, 2020; Accepted October 08, 2020

Abstract This study was carried out on the Pang catchment as a representative of the Thames River basin in the southeast of England, UK. The basin receives an average of 690 mm rainfall per year, making it one of the driest parts of the UK. Two-thirds of the basin is permeable chalk, middle Jurassic limestones, and river gravels. The Chalk is the main aquifer in southeast England. The aim of this study was to investigate the impact of climate and land-use changes on water resources. The UKCP09 climate scenarios up to 2099 were applied. The results indicated that by the 2080s, under high emission scenarios, streamflow could decrease by 37%, 32%, and 70% during summer-autumn, winter and spring, respectively while the groundwater recharge could decrease by 70% and 46% during summer-autumn and winter-spring, respectively. Increasing broadleaf forest area would reduce streamflow and groundwater recharge by 15% and 19% during spring and summer, respectively. The Reconnaissance Drought Index, RDI projected an increase in number, severity, and frequency of drought events up to the 2080s. The results of the Pang would help in future regional planning and management of the water resources in the southeast of England.

Keywords: DiCaSM hydrological model, climate change, land use change, pang catchment, water resources management

Cite This Article: Afzal M., and R. Ragab, "Impact of the Future Climate and Land Use Changes on the Hydrology and Water Resources in South East England, UK." *American Journal of Water Resources*, vol. 8, no. 5 (2020): 218-231. doi: 10.12691/ajwr-8-5-2.

1. Introduction

Given the continuous global population increase, water resources are coming under increasing pressure. In addition to population increase, there are other factors that exert pressure on water resources, such as climate and land use changes [1]. Streamflow and groundwater recharge strongly depend on climate and land use practices. The prospect of drier summers and wetter winters in the UK, due to climate change, would have significant impact on water resources, especially where the water requirements of the urban and rural communities must be carefully managed in order to protect and preserve the natural ecosystem [2].

The potential impact of the land use changes on the streamflow takes place due to differences in evaporation and transpiration rates from different types of vegetation and the difference in the rooting depth [3]. In a study [4] on the impact of land cover changes over 1508 catchments across the world. They found that the land cover made an important contribution in the water balance. Studies in a Northern England catchment [5] found an increase of runoff by ploughing upland grass area of a small catchment and a decrease in number of trees also resulted

in increased runoff. The other factor which could affect the hydrological cycle is the urban expansion due to the changes from vegetated to impermeable surfaces, which often results in increased runoff [6]. Most of the studies suggested that the impact of land use changes is more evident on small catchments, such as the Pang catchment.

The definition of drought varies from one country to another, due to the complexity of drought phenomena, difference in hydro-climatic conditions and catchment characteristics. For that reason, there is a lack of a universal drought index for assessing drought conditions in a certain region. There is a need to conduct an evaluation of different drought indices in order to identify a suitable drought index for a certain region.

In a previous study [7], indices were compared for their ability to predict agricultural drought impacts in the UK. They selected two of the most commonly used drought indices, the Standardized Precipitation Index SPI which represents the deviation from long-term average precipitation and the Standardized Precipitation-Evaporation Index, SPEI for the period 1975-2012. They found that the SPEI is the best indicator to predict the probability of drought impacts on agriculture in the UK. Assessment of the performance of five drought indices [8] for a semi-arid basin in western India for the period of 25

years (1985-2009) was carried out. They concluded that SPEI is the most suitable drought index for monitoring drought conditions.

In Iran, [9] used meteorological data of 22 synoptic stations with different climatic conditions during 1967-2014 to calculate the Reconnaissance Drought Index, RDI which represents the ratio of total rainfall to total potential evapotranspiration and the effective Reconnaissance Drought Index, eRDI, which uses effective rainfall. They found that in stations with humid condition, difference between RDI and eRDI indices were not significant, but in stations with hyper-arid and arid condition, the difference was significant.

The Pang catchment has special significance as it has been subjected to drought in the past and could be at further risk in the future, due to climate and land use changes. As there was no comprehensive study conducted on this low land catchment, the main aim of this study is to assess the impact of climate and land use changes on surface and ground water resources and to identify the relevant drought indices for meteorological, hydrological and agricultural droughts under current and future climate conditions.

The model selected for this study is the Distributed Catchment Scale model, DiCaSM [10]. The model has been successfully applied on catchments in Brazil [11,12], in Italy, [13] and in Cyprus [14]. The results suggested that the DiCaSM model could be used as an effective tool

for water authorities and decision makers to help balance future water demand and supply.

2. The Catchment, Data and the Methodology

2.1. The Pang Catchment

The Pang catchment is situated in the eastern part of the Berkshire-Marlborough Downs, England, UK (Figure 1), and the stream flow gauging station is at Pangbourne. The NRFA reference number is 39027 with the catchment area of 170.9 km². The average annual rainfall between 1961 and 1990 (baseline data) was 695 mm, while the average rainfall for the period 1961-2012 was slightly over 700 mm. River flow data were available from 1968. Before 1993 the runoff of the catchment was substantially reduced by groundwater abstractions by the Compton pumping station at Compton. The catchment is a representative of typical Southern England chalk lowland, with river flows that are dominated by slow responding groundwater. The catchment experienced a number of drought events, including the 1975-77, 1991-92, 1995-97, 2004-06, 2010-12 and 2018 drought events. The key land cover comprises woodland 16%, arable and horticultural land 51%, grass 29% and urban 4% (Figure 2).

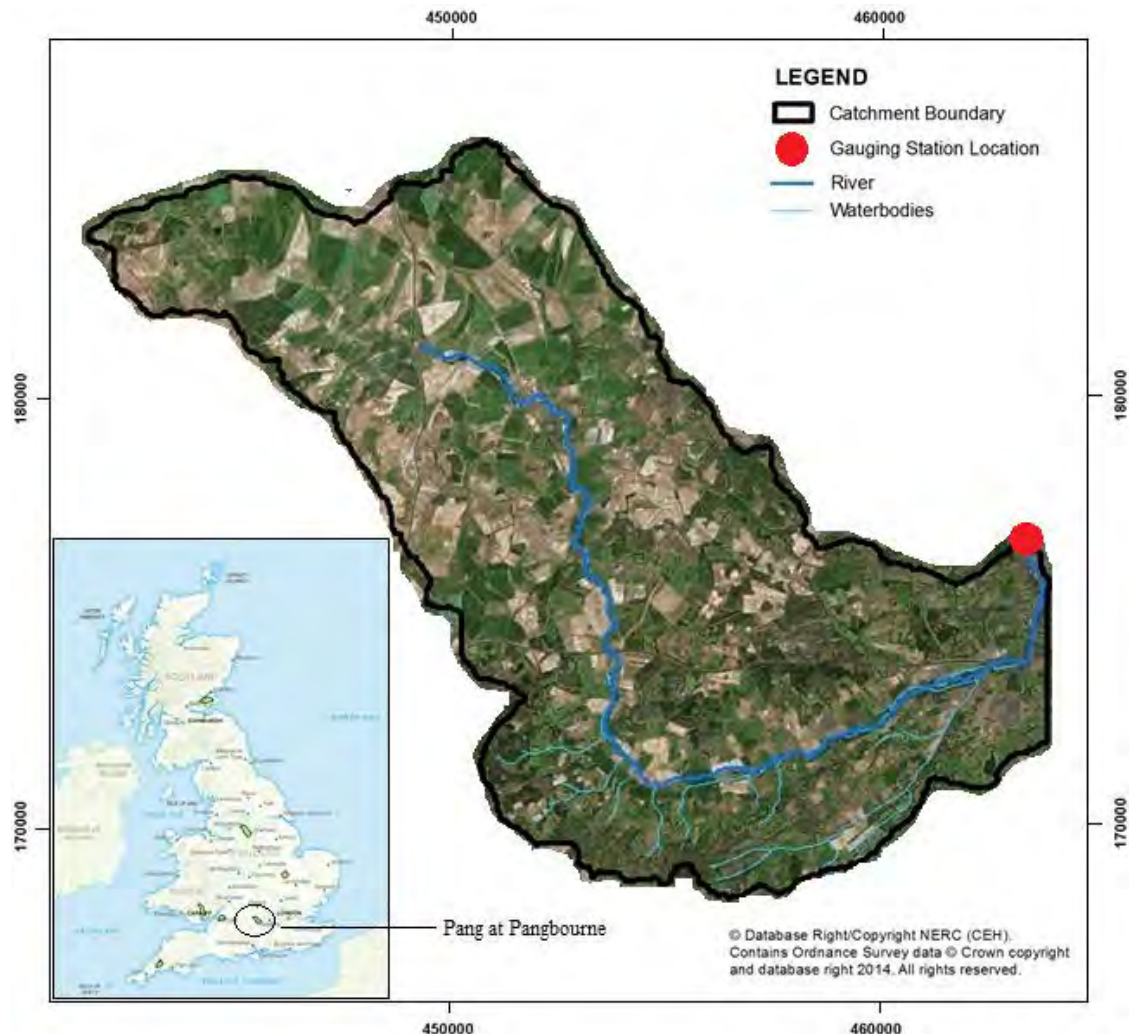


Figure 1. The boundary of the Pang catchment and the location of the gauging station at Pangbourne, Berkshire, adapted from [15]

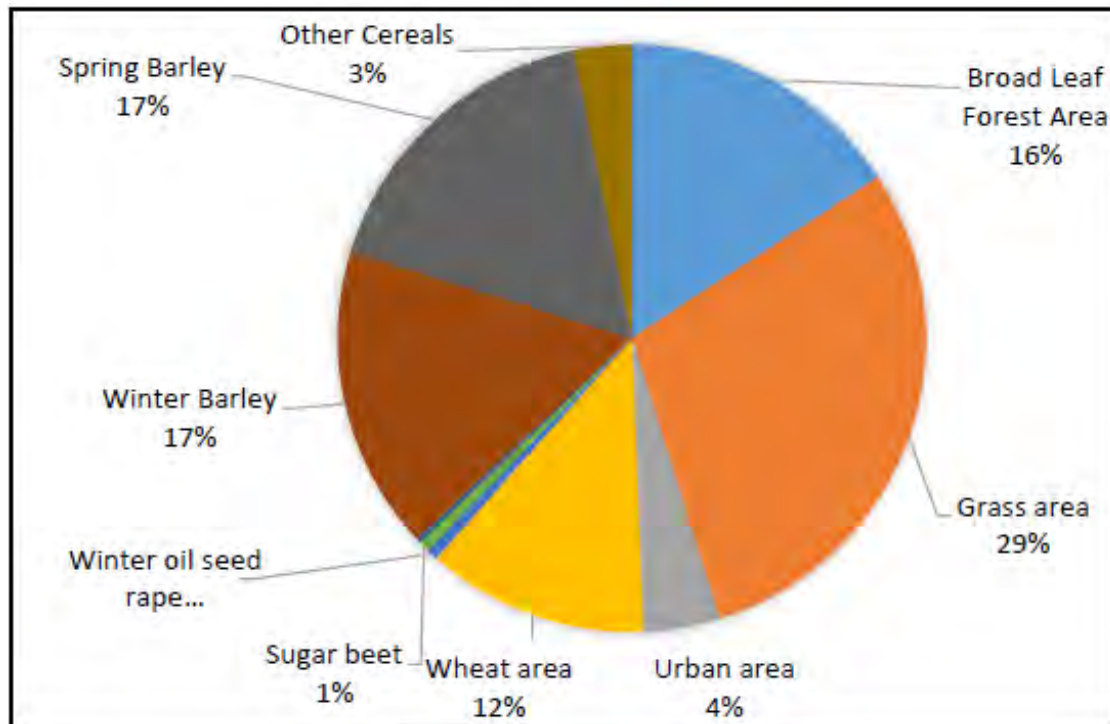


Figure 2. Current land use in the Pang catchment

2.2. The Modelling Input Data

For the modelling study, the physically based Distributed Catchment Scale Model, DiCaSM, was selected. The catchment was divided into 218 grid squares, each of which has an area of 1 km². The model was run on daily time step. The model input requires daily data of precipitation, temperature, wind speed, net radiation or total radiation and vapour pressure. The rainfall is a key input for runoff generation calculation while temperature, radiation, vapour pressure and wind speed are essential to calculate the evapotranspiration. Climate data were obtained from the Climate, Hydrology and Ecology research Support System (*CHES*) for 1962 until 2012 period. The catchment boundary and gauging station location were collected from Centre for Ecology and Hydrology [16] and [17] and the National River Flow Archive provided data for the daily river flow for the Pang catchment [18]. The naturalized river flow data (1979-2012) were obtained from the UK Environment Agency, EA. The data were

used to calibrate and validated the stream flow predicted by the model. The UK Land Cover data were obtained from the Centre for Ecology and Hydrology (Land Cover Map 2007 (25m raster, GB) Web Map Service [15]). The map was used to provide the relative area of each land cover type within each grid square of the catchment. The data were used to calculate the evapotranspiration of each land cover type. The soil data were obtained from Cranfield University (1:250 000 Soilscales for England and Wales Web Map Service). The soil properties data were used to calculate the infiltration of water through the soil surface, water movement between the soil layers, drainage, recharge, soil water storage and availability for plants. The digital elevation model (DEM) was available from CEH data archive. The data were used to generate the elevation of each grid square and subsequently used to calculate the slopes and the surface flow directions. Plant parameters obtained from the UK Meteorological Office MORECS system that has a database for UK land covers and were used for evapotranspiration calculations.

Table 1. Probabilistic changes in temperature and precipitation for the Pang catchment using the joint probability of the UKCP09 climate change scenarios for low, medium and high emission scenarios for the 2020s, 2050s and 2080s (30-year time periods).

		Low emissions				Medium emissions				High emissions			
		Winter	Spring	Summer	Autumn	Winter	Spring	Summer	Autumn	Winter	Spring	Summer	Autumn
Change in precipitation (%)	2020s	5.85	3.09	-4.36	3.43	5.44	2.39	-6.85	2.42	6.43	2.28	-3.73	0.97
	2050s	10.66	2.10	-19.22	1.97	12.28	1.37	-16.91	5.54	14.16	1.49	-16.79	4.80
	2080s	15.21	2.62	-13.63	2.81	19.96	2.32	-20.96	5.62	28.30	2.41	-27.59	5.40
Change in temperature (°C)	2020s	1.29	1.26	1.65	1.64	1.36	1.28	1.49	1.60	1.35	1.26	1.49	1.65
	2050s	1.99	1.78	2.73	2.31	2.09	2.07	2.62	2.72	2.48	2.32	3.03	2.95
	2080s	2.57	2.31	2.80	2.96	2.86	2.85	3.59	3.53	3.55	3.66	4.73	4.69

To study the impact of future climatic change on water resources, the UK Climate Projection Scenarios (UKCP09) were used, using the joint probability factors and the weather generator data. In this study three 30-year periods: 2020's (2010-2039), 2050's (2040-2069) and 2080's (2070-2099) for the three greenhouse gas emission scenarios (low, medium and high) were considered. The UKCP09 provides monthly, seasonal and annual, probabilistic changes factors at 25 km by 25 km grid square resolution for precipitation and temperature (Table 1). The seasonal temperature shows an increase with emissions scenario and time, particularly in summer and autumn, whereas the precipitation is showing rainfall decreases in summer and increases in winter relative to the 1961-1990 'baseline' period. The weather generator, WG, provides daily output data at a 5km² resolution for more climate variables, such as vapour pressure and sunshine hours, in addition to rainfall and temperature. The sunshine hours were converted into net radiation [19]. The simplified change factors were derived from UKCP09 joint probability central estimates. Climate change data were input to the DiCaSM model.

2.3. Catchment Characteristics

The Pang catchment is located in a drier part of the UK and often experiences low river flow. Before 1993, the catchment has been under severe abstraction of surface and groundwater [20].

2.4. The DiCaSM Model

This study applied the DiCaSM hydrological model which is the acronym for the Distributed Catchment Scale Model [10,14]. The model is physically based and considers the commonly known hydrological processes such as rainfall interception, infiltration, evapotranspiration, surface runoff to streams, recharge to groundwater, water uptake by plants, soil moisture dynamics, and stream flow. The model adopts a distributed approach with variable spatial scale (default is 1km grid square) and requires daily input data of rainfall, temperature, wind speed, vapour pressure, and total or net radiation and runs on a daily time step.

2.4.1. The Components of the DiCaSM Model

The rainfall interception by grass was calculated using the equations reported in [21], by crops according to [22], and by the trees according to [23]. Potential evapotranspiration of mixed vegetation was calculated according to [24] whereas the surface runoff calculation was based on either excess saturation or excess infiltration. The infiltration was calculated according to either [25] or [26] equations. The runoff is routed between the low points of each grid square along the prevailing slope using the digital terrain model (DTM). The model calculates soil water balance of the root zone based on the four layers model [27] and calculates overland and channel flow according to [28]. Further details about the model are given in [14] and [10].

2.4.2. Model Performance Indicators

To determine the model efficiency/goodness of fit, the simulated and observed flow data were compared using a number of indices, including the Nash-Sutcliffe Efficiency (*NSE*) coefficient. [29] A *NSE* coefficient of 1 or 100% indicates a perfect match.

$$NSE = 1 - \frac{\sum_{i=1}^n (O_i - S_i)^2}{\sum_{i=1}^n (O_i - \bar{O})^2} \quad (1)$$

where O_i and S_i refer to the observed and simulated flow data, respectively, and \bar{O} is the mean of the observed data.

The calibration procedure consisted of adjusting the stream flow relevant parameters to achieve the best model fit with the latter assessed using the *NSE* values.

The extreme values in a time series can result in a poor *NSE* values [30]. For this reason, they suggested calculating the *NSE* with natural logarithmic values:

$$\ln NSE = 1 - \frac{\sum_{i=1}^n (\ln O_i - \ln S_i)^2}{\sum_{i=1}^n (\ln O_i - \ln \bar{O})^2} \quad (2)$$

In addition, the model performance can be evaluated using the coefficient of determination, R^2 as:

$$R^2 = \left(\frac{1}{N} \frac{\sum (y_o - \bar{y}_o)(y_s - \bar{y}_s)}{\sigma_{y_o} - \sigma_{y_s}} \right) \quad (3)$$

where y_o is the observed value, y_s is the simulated value, N is the total number of observations, \bar{y}_o is the average measured value, \bar{y}_s is the average simulated value, σ_{y_o} is the observed data standard deviation and σ_{y_s} is the simulated data standard deviation.

2.5. Identification of Drought Indices

Using a range of drought indices helps in identifying different types of droughts. The most commonly used index is the Standardized Precipitation Index (*SPI*) [31]. The index represents the deviation of precipitation from the long-term average, where negative values indicate "dry periods" and positive values indicate "wet periods". The *SPI* index is relevant for meteorological, agricultural and hydrological drought, as precipitation is the key climatic variable upon which soil moisture deficit, stream flow and groundwater recharge depend. The *SPI* could be used to quantify the severity of both dry and wet events. The *SPI* index scale values mean: above 2.0 extremely wet, 1.5-1.99 very wet, 1.0-1.49 moderately wet, -0.99 to 0.99 near normal, -1.0 to -1.49 moderately dry, -1.5 to -1.99 severely dry and -2.0 and less, extremely dry.

The other key drought index used in the study was Reconnaissance Drought Index (*RDI*) according to [32]. The index is calculated using the ratio of precipitation to potential evapotranspiration over a certain period. The Reconnaissance Drought Index (*RDI*) was calculated as:

$$a_0^{(i)} = \frac{\sum_{j=1}^{12} P_{ij}}{\sum_{j=1}^{12} PET_{ij} \text{ or } AE_{ij}} \quad (4)$$

$$RDI_n^i = \frac{a_0^{(i)}}{\bar{a}_0} - 1 \quad (5)$$

$$RDI_{st(k)}^i = \frac{y_k^{(i)} - \bar{y}_k}{\hat{\sigma}_{yk}} \quad (6)$$

where P_{ij} and PET_{ij} are the precipitation and potential evapotranspiration of the j_{th} month of the i_{th} hydrological year (starting from October), \bar{a}_0 is the arithmetic mean of the a_0 calculated for the number of years, y_i is the $\ln(a_0^{(i)})$, \bar{y}_k is its arithmetic mean and $\hat{\sigma}_{yk}$ is its standard deviation. The RDI has been used in studies in Greece [33] and in Iran and Iraq [34].

An adjusted RDI was also calculated, using the net rainfall (gross rainfall minus rainfall interception losses by canopy cover) and actual evapotranspiration. The RDI index scale values mean: above 2.0 extremely wet, 1.5-1.99 very wet, 1.0 -1.49 moderately wet, -0.99 to 0.99 near normal, -1.0 to -1.49 moderately dry, -1.5 to -1.99 severely dry and -2.0 and less extremely dry [35].

The adjusted RDI is not commonly used due to limited availability of actual evapotranspiration and net rainfall data. The DiCaSM model provides actual evaporation as well as net rainfall (after deducting the rainfall intercepted by land cover from the total rainfall). Therefore, the RDI and the adjusted RDI can be calculated from the model output. Both RDI and the adjusted RDI have advantage over SPI as the SPI only accounts for precipitation.

In addition, two more indices were considered, the soil moisture deficit, SMD which is widely used as a drought index relevant to agricultural drought monitoring [36] and soil wetness index for the drought monitoring [37]. A SMD of zero means, the catchment's soil moisture is at field capacity. The deviation gets larger when the soil moisture starts to fall below the field capacity, especially during summer and drought periods.

The wetness index, WI is a scaled soil moisture of the catchment and is a relevant index to detect hydrological drought, as this is commonly associated with soil moisture status of the catchment. The wetness index, WI represents how relatively wet or dry the catchment is over a period of time. A WI value of 1 means the catchment is at the maximum soil moisture and WI of zero means the catchment is at its minimum soil moisture content. The soil moisture deficit is the difference between soil moisture at field capacity and the current soil moisture. The SMD together with the RDI, identify agricultural droughts, where availability of the soil water is a key for the crop growth and alerting farmers for the need for irrigation.

3. Results

3.1. Model Calibration/Validation for the Streamflow

Streamflow data were available from 1970 to 2012,

climate data were available from 1961 to 2012. For the model calibration, the DiCaSM model depends on a number of model parameters: base flow, stream bed infiltration/leakage, the percentage of flow routed to stream, catchment storage/time lag coefficient, exponent function of the peak flow and stream storage/time lag coefficient. The model was run while tuning the above parameters using different time periods and one of the best time periods was selected for the model calibration. For the Pang, selection of the calibration period was important as river flow of the catchment is significantly affected by the ground water abstraction thus reducing the streamflow substantially. This groundwater abstraction took place until 1993. To get the best model parameters, the model was calibrated using the best available stream flow data after 1994, i.e. after Compton pumping station was closed.

A simple iteration algorithm was used for the optimization process in which each of the above-selected parameters were assigned a realistic range (minimum and maximum values). The range was divided into steps/increments. The number of iterations was the multiplication of the number of steps of all the calibration parameters. The model calculates the NSE for each iteration. An important issue in the Pang was to parameterize the extreme drought events/low flows, as streamflow is very low during the summer months, as the river mainly depends on its base flow. Therefore, the base-flow was the most sensitive parameter on which stream flow depends. Figure 3 shows that the model performed extremely well during the model calibration period of three years (2001 - 2003), the model efficiency expressed as the NSE was above 92% and $\ln NSE$ above 89%. The model performance during the model validation period was also good, with NSE and $\ln NSE$ values above 86%. The model performance was better during the 1994-2012 period, when the Compton pumping station was closed. During the model calibration stage, the percentage error between simulated and observed stream flow was around 2% (Table 2). The model calibration was carried out for a short period (Figure 3 left) followed by the validation over longer periods, from seven years to the entire available record (Figure 3 right). The model results clearly illustrate that before 1993, when water was abstracted at the Compton pumping station, the observed stream flow was always lower than the simulated values, this is because groundwater abstraction significantly affects the groundwater level and the base-flow contribution to the streamflow, especially during the dry summer months.

The model also performed reasonably well during the 1970s drought decade, but slightly overestimated, as the observed flow was affected by groundwater abstraction. The overall model performance was extremely good, whether the results of the model efficiency were calculated as NSE , $\ln NSE$ or R^2 . Figure 4 shows the model's capability to reasonably predict stream flows both during the model calibration and validation periods.

The uncertainty level in streamflow prediction was estimated using the containment ratio, CR. The latter refers to the % of observations that contained within the 95% and 5% prediction quantiles. The CR value was 87% for the period of 1993-2012 [38].

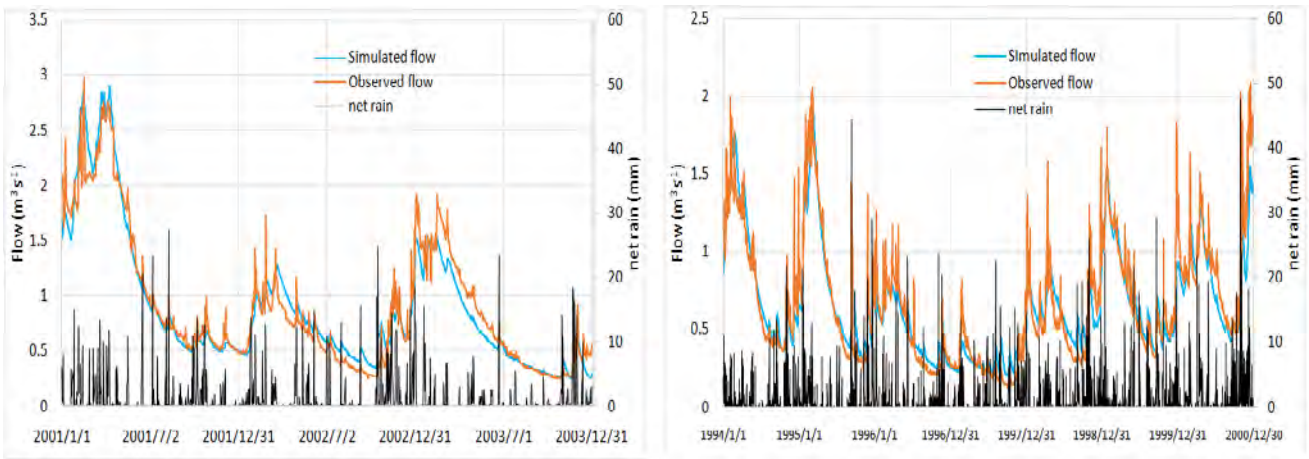


Figure 3. Model calibration for 2001-2004 (left) and validation for 1994-2002 (right)

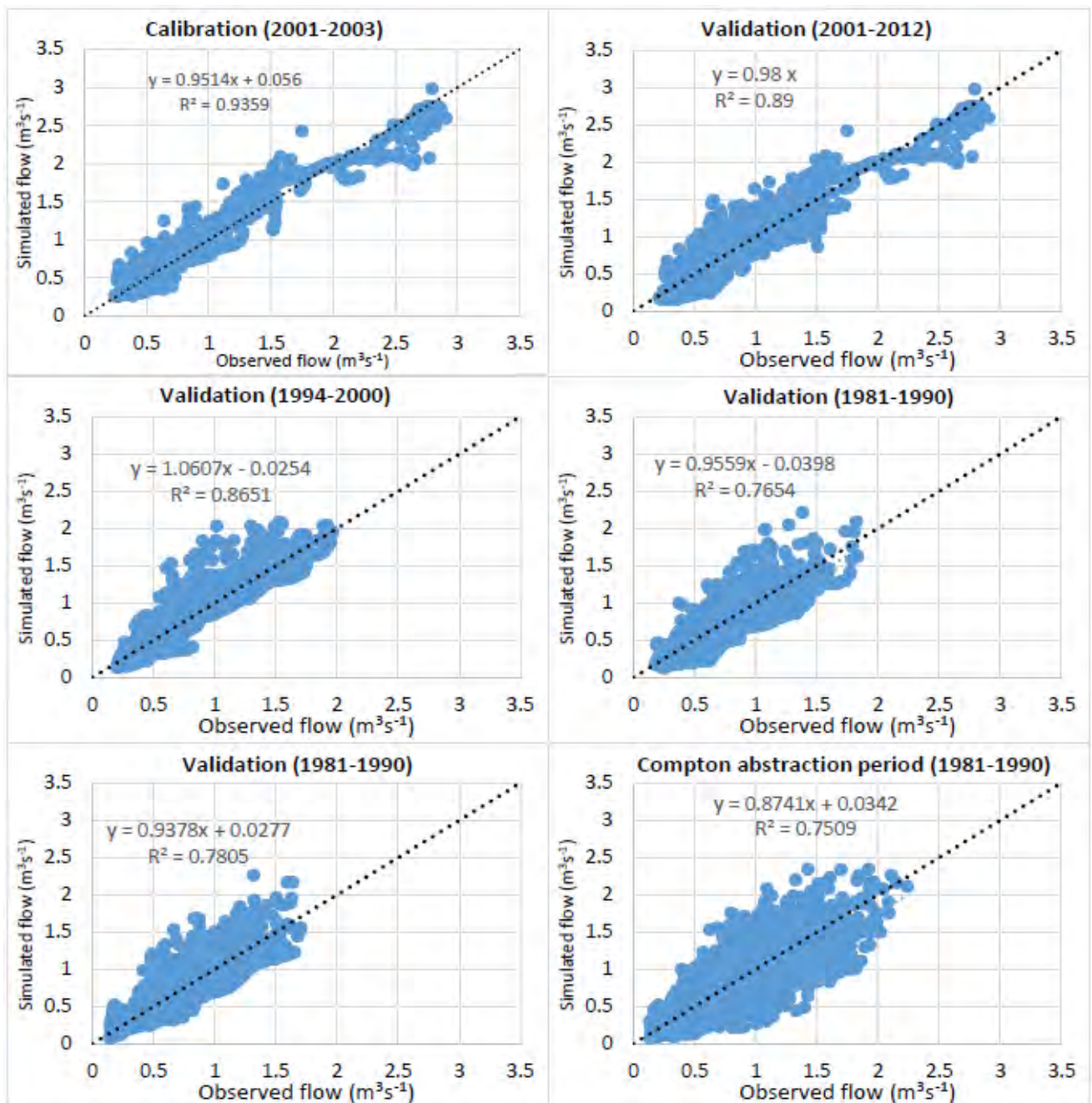


Figure 4. Relationship between observed and simulated flow during the model calibration and model validation over a decadal time scale and over the entire period

Table 2. Pang model performance during the calibration and validation stages

Periods		Process	NSE (%)	ln NSE	R ²	Modelled flow (m ³ s ⁻¹)	Observed flow (m ³ s ⁻¹)	Error %
After Compton pumping closed	2001-2003*	Calibration	92.44	89.17	0.94	0.79	0.81	-2.14%
	2001-2012	Validation	89.57	82.85	0.90	0.66	0.64	2.96
	1994-2000	Validation	86.09	86.74	0.86	0.67	0.68	-2.20
	1970-2012	Validation	80.42	80.13	0.81	0.61	0.59	3.67
Compton pumping in operation	1971-1980	Validation	77.6	79.36	0.78	0.62	0.61	1.76
	1981-1990	Validation	71.25	69.71	0.76	0.65	0.59	11.23
	1971-1993	Validation	71.12	75.72	0.74	0.62	0.58	6.90

*calibration period.

3.2. Identification of Historic Droughts

3.2.1. The Standardized Precipitation Index (SPI)

The SPI was able to identify drought events which took place in the Pang catchment between 1961 to 2012 period (Figure 5). The *SPI* drought index crossed over the line that represent the extremely severe drought level during the 1975/76 drought which affected most parts of the UK and Europe.

The *SPI* index over 52 years elucidated the successive dry events, as those that occurred in the 1970s. The *SPI* index also helped in identifying smaller magnitude drought events or drier periods which took place in the late 1960s,

the 1990s, and in 2003-2005, 2009 and 2010. Such major drought events have been reported [39]. According to the drought severity index, the 2005 and 2006 summers were the greatest droughts of the English lowlands and the South-East, where the Pang is located. The magnitude of the severity of drought was considered as severe in the early 1960s, in the mid-1970s, in 1976 and in 1990, when *SPI* was below -2.0 which is considered extremely dry.

3.2.2. Reconnaissance Drought Index (RDI)

Figure 6 shows the comparison between the *RDI* and the adjusted *RDI*. The *RDI* and adjusted *RDI* picked up all the drought events which were observed by the *SPI* index.

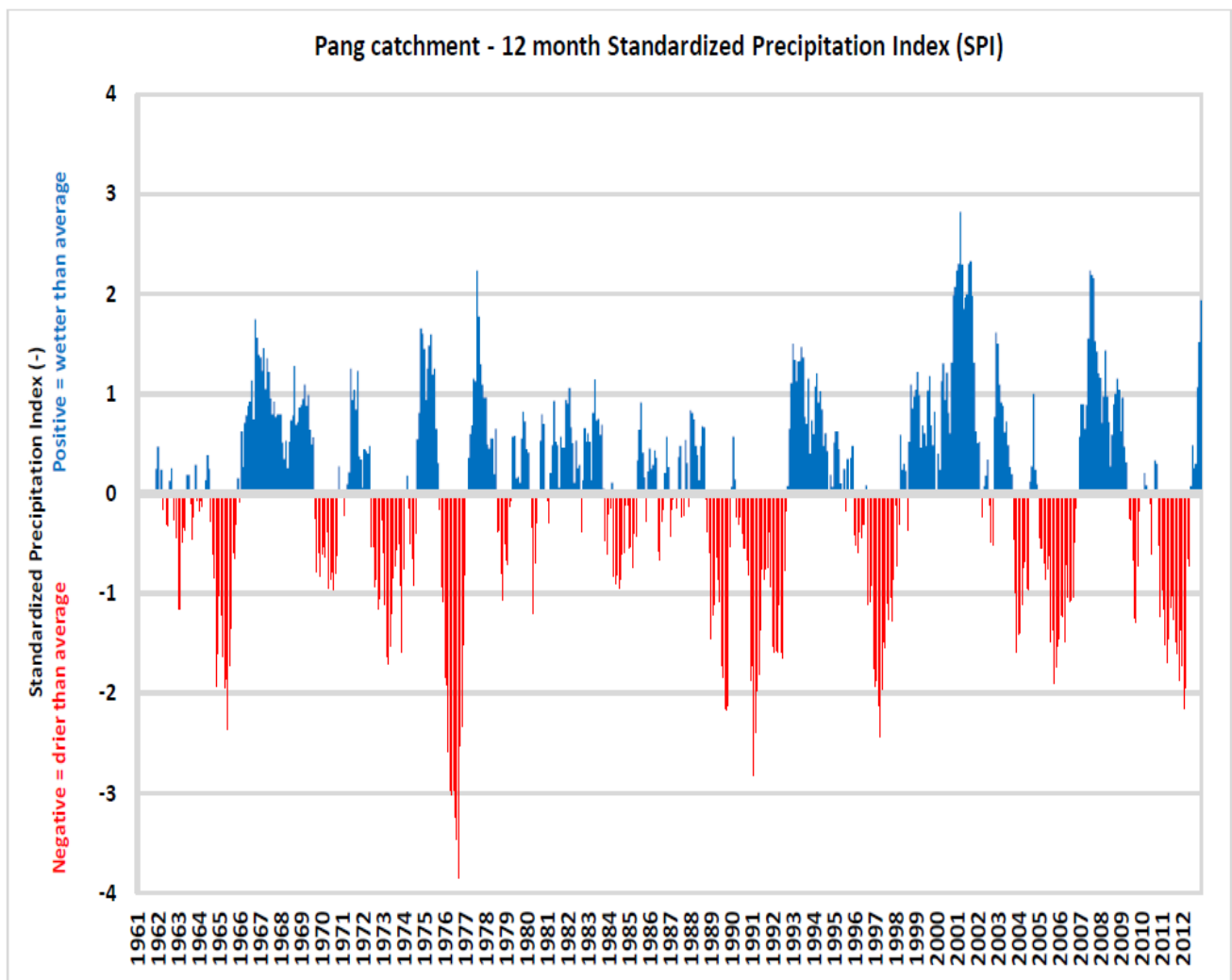


Figure 5. Twelve months standardized precipitation index (*SPI*) for the Pang catchment from 1961-2012

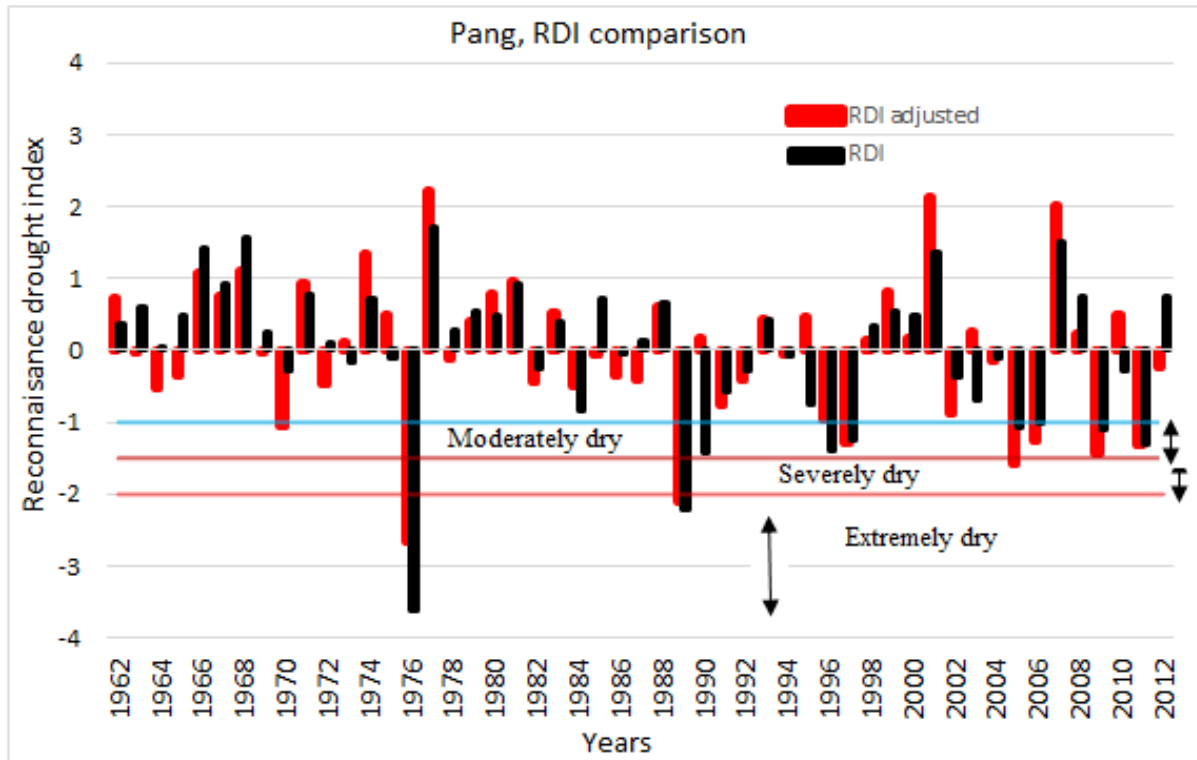


Figure 6. Historic RDI and adjusted RDI for the Pang catchment for the period 1962-2012

The adjusted *RDI* showed slightly different severity levels, especially during the extreme drought events, when compared with the *RDI* index. There is a strong correlation between the *RDI* and the *SPI*. Figure 5 and Figure 6 show that extreme drought conditions were observed in 1976, as *SPI*, adjusted *RDI* and *RDI* reached a low value of extreme drought level. Drier than average spells (*SPI* less than -10% or *RDI* less than -1) were also observed in 1990, 1996, 1997, 2005, 2006, and 2009 and 2011. The two major drought events of 1976 and 1989 were detected by both the *SPI* and *RDI* drought indices.

3.2.3. Soil Moisture Deficit, SMD and Soil Wetness Index, WI as Drought Indicators

Figure 7 shows the *WI* and *SMD* during the dry summer

months. In the dry summer months of 1976, the soil moisture deficit reached 208 mm and during the 1975 dry summer period, soil moisture deficit reached 150 mm. The figure also shows that the severity of the dry event of summer 1976 was a result of the dry winter of the 1975-1976, as the *SMD* did not drop down to zero as expected in winter. In contrast, the 1977 winter months received above average rainfall that brought the *SMD* back to zero. It can also be seen that the *WI* dropped down below the winter value of 1.0 to 0.04 during the extreme drought of the summer of 1976, and the *SMD* mirrored the trend of the *WI*. This suggests that the severity of the 1976 drought reached to a very extreme level during the summer season. Each of the drought indices identified the 1970s drought as severe drought.

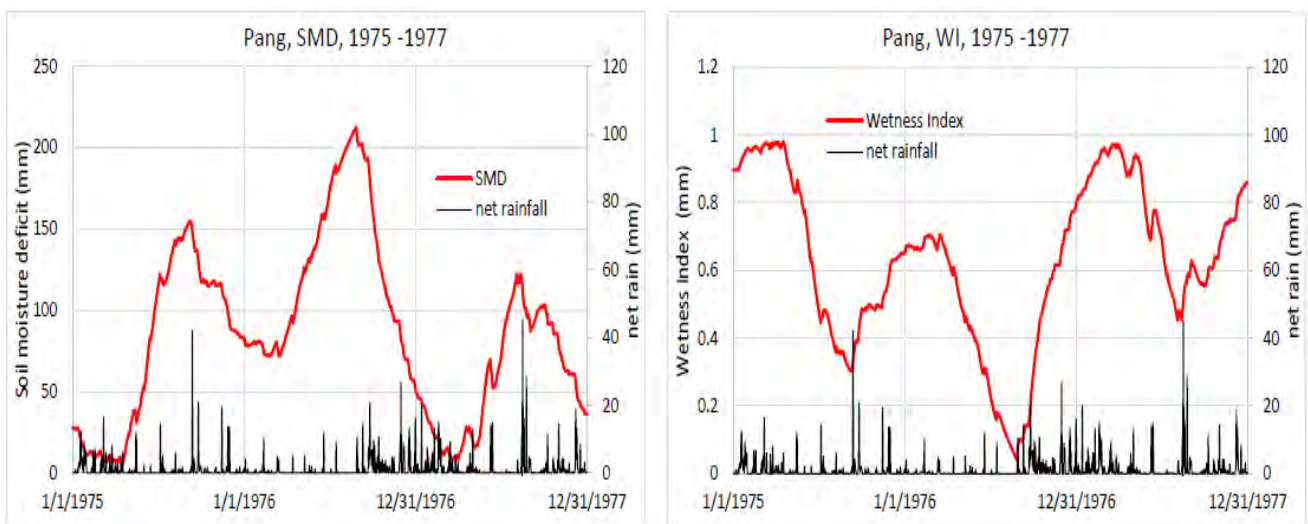


Figure 7. Soil moisture deficit (SMD) and the Wetness Index (WI) at root-zone for the Pang catchment during the period 1975-1977

3.3. Future Hydrological Changes and the Drought Indices

3.3.1. Changes in Streamflow

Under all future emission scenarios of the UKCP09, the expectation is a strong likelihood of more wintery rainfall, lower summer rainfall and higher summer temperatures. The effect of low summer rainfall and higher temperature will have more impact in the south east of the UK. In the current study, climate change scenarios were developed using two approaches based on UKCP09 outputs: simplified change factors based on joint probability data and the weather generator data. Three 30-year periods: 2020's (2010-2039), 2050's (2040-2069) and 2080's (2070-2099) for the three greenhouse gas emission scenarios (low, medium and high) were considered.

Using the joint probability approach, the seasonal climate change factors of temperature (\pm change in $^{\circ}\text{C}$) and rainfall (% change in rainfall) at the most likelihood probability level were input to the DiCaSM model and applied to the 1961-1990 baseline climate data (Table 1). The weather generator data of temperature, rainfall, vapour pressure and radiation for 100 realizations of each 30 years' period were employed in the DiCaSM model as a daily input of the three time periods and the three emission levels. The streamflow projections under both the simplified change factors suggest that the stream flow is more likely to be reduced under all emission scenarios without any exception (Table 3).

Under all emission scenarios, the summer streamflow is likely to decrease by 15.6 % to 21.6% in the 2020s, by 27.9% to 36.7% in 2050s and by 32.7% to 46.6% in 2080s when using the joint probability factors and by 18.0% to 19.7% in the 2020s, 18.0% to 27.6% in the 2050s and 19.2% to 27.7 % in the 2080s when using the weather generator data. A significant decrease in stream flow is projected in the 2050s and 2080s summer under all emission scenarios, more particularly under the high emission scenario.

This decrease in streamflow is likely to continue during the autumn when flow could decrease by up to 36.8 % and 29.7% in the 2080s when applying UKCP09 joint probability and weather generator data under high emission scenarios for the 2080s, respectively. Although, a consistent pattern of streamflow decrease was found in

all seasons, using both UKCP09 joint probability factor and weather generator data, the severity of the decrease was mostly higher when using joint probability factors than when using the weather generator data. The severity of the change, particularly during the summer season, could lead to very low stream flows, possibly leading to a high risk of inadequate domestic, environmental and agricultural water supply.

3.3.2. Changes in Groundwater Recharge

The DiCaSM model results show that groundwater recharge is likely to decrease in all seasons and the selected study periods, under the three emission scenarios (Table 4). The decrease gets greater with time and emission level with 2080s high emission showing the largest decrease in groundwater recharge. This decrease was generally higher when using joint probability factors than when using the weather generator data.

Although the UKCP09 projects an increase in winter precipitation, this would be counterbalanced by the higher water losses due to the increased temperature, evapotranspiration and soil moisture deficit, which result in a significant decrease in groundwater recharge. During the spring season, under all emission scenarios, a likely decrease in groundwater recharge is projected for all selected time periods. This decrease is likely to continue in the summer months due to low summer precipitation and increasing temperature, evapotranspiration and soil moisture deficit. The groundwater recharge could decrease by up to 72% under high emission scenarios of the 2080s when using joint probability factors. However, the groundwater recharge decrease was below 50% when using the UKCP09 weather generator data. It was suggested [40] that the drier summers could also lead to increased soil moisture deficit extending into the autumn and could shorten the winter recharge season. Considering an increase in winter rainfall, as projected under all emission scenarios, one would expect an increase in groundwater recharge but this might not happen as future winter precipitation is expected to come as extreme events and over a short period of time, as reported [41] and would result in increased soil moisture deficit and water losses due to the evapotranspiration and less recharge. The results shown in Table 4 clearly support this finding, as under all emission scenarios the groundwater recharge is likely to decrease for all future time periods.

Table 3. Future changes in streamflow observed using joint probability and the daily weather generator data output from the UKCP09

Scenarios	Season	% change (joint probability)			% change (weather generator)		
		Low emission	Medium emission	High emission	Low emission	Medium emission	High emission
2020s	Winter	-12.5	-16.3	-17.5	-10.8	-18.3	-18.7
	Spring	-11.8	-16.3	-17.3	-14.1	-16.4	-16.1
	Summer	-15.6	-21.0	-21.6	-18.1	-19.7	-19.2
	Autumn	-11.7	-16.7	-18.1	-22.4	-22.5	-24.0
2050s	Winter	-19.0	-21.9	-24.0	-10.1	-16.7	-19.5
	Spring	-20.2	-23.0	-26.1	-10.7	-13.6	-17.7
	Summer	-27.9	-32.5	-36.7	-18.0	-22.3	-27.6
	Autumn	-24.3	-25.1	-27.4	-24.2	-24.6	-28.8
2080s	Winter	-21.4	-27.2	-31.0	-11.5	-18.5	-24.0
	Spring	-23.6	-28.6	-32.5	-14.5	-19.0	-23.9
	Summer	-32.7	-40.6	-46.6	-19.2	-24.3	-27.7
	Autumn	-26.3	-31.6	-36.8	-25.1	-26.4	-29.7

Table 4. Future changes in groundwater recharge observed using the probabilistic change factors and using the daily weather generator data output from the UKCP09

Scenarios	Season	% change (joint probability)			% change (weather generator)		
		Low emission	Medium emission	High emission	Low emission	Medium emission	High emission
2020s	Winter	-16.9	-21.2	-24.0	-21.2	-19.2	-21.3
	Spring	-17.4	-24.2	-25.7	-15.5	-20.0	-19.5
	Summer	-31.5	-41.1	-36.1	-30.9	-32.9	-34.6
	Autumn	-25.9	-36.4	-35.8	-30.9	-31.7	-34.4
2050s	Winter	-28.0	-30.4	-34.3	-21.8	-25.5	-32.8
	Spring	-32.9	-34.7	-41.7	-19.3	-20.0	-21.7
	Summer	-52.8	-58.7	-62.3	-36.6	-35.5	-43.9
	Autumn	-50.6	-52.6	-54.5	-30.8	-35.8	-39.3
2080s	Winter	-28.7	-39.6	-46.3	-24.3	-28.0	-38.2
	Spring	-37.9	-42.2	-46.6	-17.8	-28.2	-33.6
	Summer	-56.9	-66.3	-71.7	-40.4	-44.6	-48.2
	Autumn	-55.0	-62.9	-70.2	-40.0	-44.7	-48.2

3.3.3. Drought Indices

As projected under different climate change scenarios, the decrease in rainfall and increase in temperature would likely result in an increase of soil moisture deficit and increase in evapotranspiration (Figure 8). Under climate change projections, the soil moisture is showing an increase in SMD. The SMD and evapotranspiration are projected to increase with time and with the emission level being the highest in the 2080s under the high emission scenario.

To quantify the impact of decreasing rainfall and increasing water losses due to the evapotranspiration, the standardised reconnaissance drought index, *RDI* was applied.

The *RDI* for the three selected time periods and three emission scenarios is shown in Figure 9. Generally, the number of drought events increased with time and with emission level. Under low emission scenarios, the moderate drought events increased by three times in the 2050s and 2080s, in comparison to the baseline period. A slight change in precipitation and temperature was predicted to result in moderate droughts under

the low emission scenarios for the 2020s, 2050s and 2080s. Under medium emission scenarios, the number of drought events increased from the 2020s to the 2050s to the 2080s, combined with more severe and extreme events. In the 2080s, medium emission, in total seven drought events took, place which was almost double the number of the baseline period. In comparison to the medium emission scenarios, the number of extreme drought events increased with time under high emission scenarios due to the decrease in rainfall and increase in temperature which resulted in higher water losses by evapotranspiration which, in turn, resulted in higher severity of drought events. Although in the 2050s, under high emission scenarios, seven significant (2 extreme, 3 severe and 2 moderate) drought events are projected, the number and severity of the drought events (eight) was higher in the 2080s (3 extreme, 2 severe and 3 moderate). In the 2080s, under high emission scenarios, three extreme drought events were projected due to warmer climatic conditions, especially in the summer and autumn seasons using the UKCP09 weather generator data.

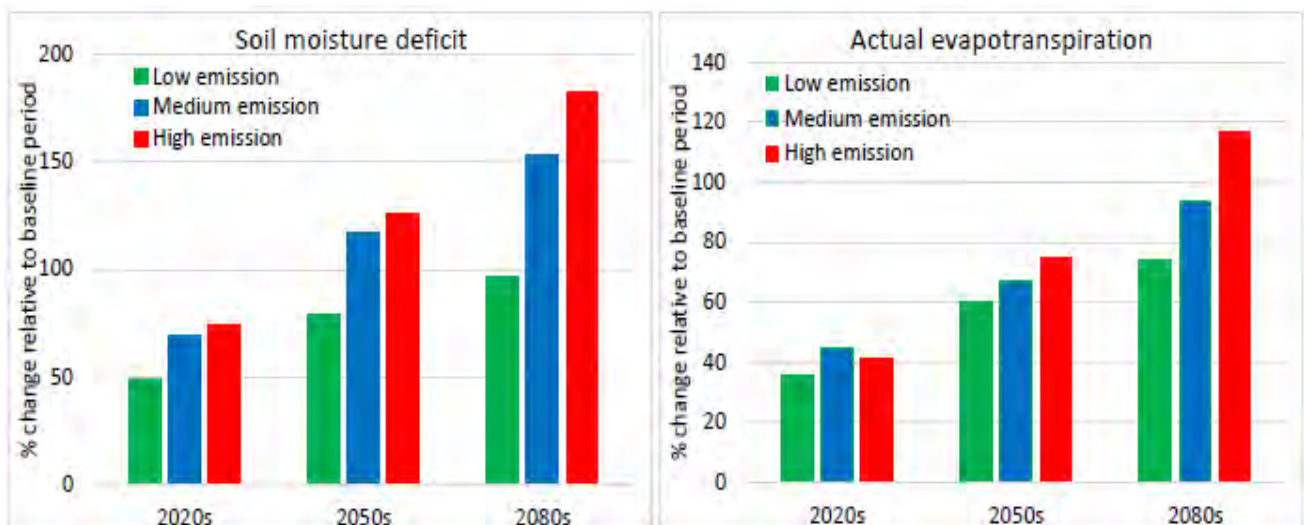


Figure 8. Seasonal changes in soil moisture deficit and actual evapotranspiration in the Pang catchment under all emission scenarios based on UKCP09 joint probability factors

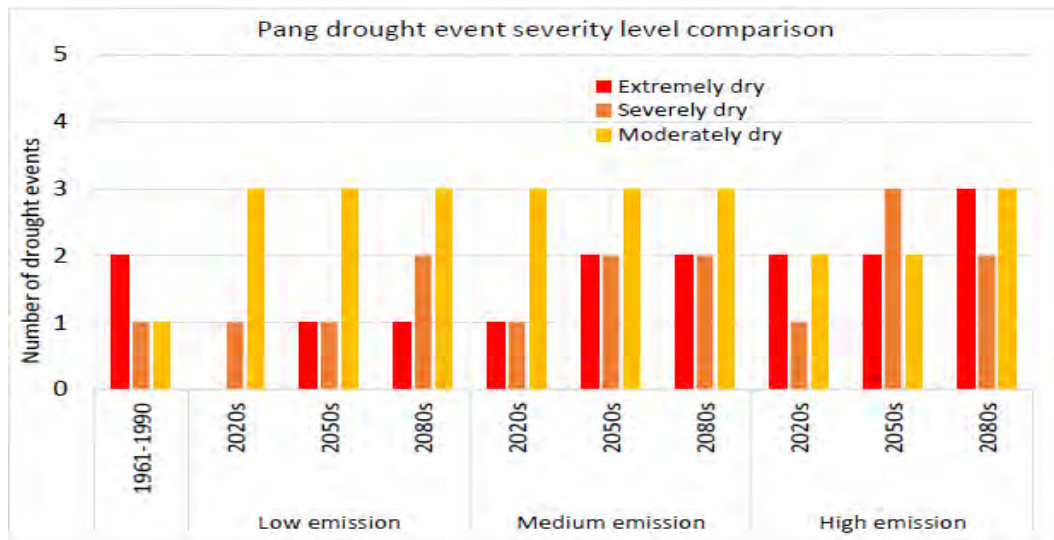


Figure 9. Severity of the annual drought events observed using the Reconnaissance Drought Index (RDI) season under all emission scenarios using the weather generator data

3.4. Impacts of Land Use Changes on the Water Resources

To study the impact of land use changes, a number of plausible (stakeholders’ input) and hypothetical land use scenarios were created. Not only the rainfall interception, water uptake and water evapotranspiration change the water balance but also temporal dynamics of the plant cover during the growth stages have significant impact on the initiation of the surface runoff and consequently the streamflow and the groundwater recharge. Results of possible land-use changes and the impact of the land use changes on the streamflow, groundwater recharge, soil moisture deficit, and the evapotranspiration are listed in Table 5. The evapotranspiration significantly affects the surface runoff from April to September as this period is the fastest growth stage of vegetation. The plants reach their maximum canopy cover, or Leaf Area Index, *LAI* during this period. The water losses by

evapotranspiration are positively correlated with the *LAI* and canopy height, which are increasing during the April to September period. The possible and the hypothetical land use changes showed a varying impact on the selected hydrological variables, the river flow, the groundwater recharge, soil moisture deficit and the actual evapotranspiration.

The expansion of the wood broadleaf forest would likely result in decreasing stream flow by 12.4%, 16.6%, 14.4% and 9.0% during winter, spring, summer and autumn, respectively, while the groundwater recharge would decrease by 13.5%, 15.2%, 21.9%, and 9.6% during winter, spring, summer and autumn, respectively. The summer soil moisture deficit and evapotranspiration increased by 44.5% and 53.9%, respectively. The increase in soil moisture deficit, more specifically during the spring and summer seasons are due to the fact that the plant growth reaches its maximum, and plants take up and transpire water at maximum rate during this period.

Table 5. Impact of land use changes in the Pang catchment on selected hydrological variables

Hydrological variables	Land use types						
	100% Grass area replaced by winter barley	Grass area replaced by oil seed rape	40% urban expansion replacing grass and arable area	Replacing 50% of winter barley by oil seed rape	Whole catchment as grass area	Whole catchment as Broad leaf forest area	
	Season	%	% change	% change	% change	% change	
River flow	Winter	6.46	-2.8	1.14	-1.35	-2.64	-12.4
	Spring	6.10	-1.2	1.13	-0.50	-5.22	-16.6
	Summer	3.39	-0.31	0.42	-0.10	-8.35	-14.4
	Autumn	3.57	2.4	-0.05	-1.14	-3.90	-9.01
Groundwater recharge	Winter	6.53	-2.01	1.40	-0.47	-7.80	-13.48
	Spring	5.21	-0.05	1.90	0.30	-6.10	-15.21
	Summer	0.60	-1.95	1.40	0.58	-9.10	-21.90
	Autumn	6.48	3.91	1.80	-3.13	-5.30	-9.65
Soil Moisture Deficit	Winter	-14.5	0.97	-14.8	0.46	13.65	2.1
	Spring	-12.1	2.19	-12.8	0.46	5.67	13.1
	Summer	-1.9	3.13	-6.70	0.86	11.76	44.5
	Autumn	-4.6	0.45	-7.3	0.28	6.41	13.6
Actual Evapotranspiration	Winter	-8.3	1.17	-10.2	0.91	11.28	4.64
	Spring	-6.9	2.65	-8.80	0.91	4.69	15.80
	Summer	-1.1	3.78	-4.6	1.72	9.72	53.87
	Autumn	-2.6	0.54	-5.0	0.56	5.30	16.51

Changing grass area by winter barley led to a small increase in stream flow and groundwater recharge. Stream flow increased by 6.5%, 6.1%, 3.4% and 3.6% during winter, spring, summer and autumn, respectively. At the same time, the groundwater recharge increased by 6.5%, 5.2%, 0.6% and 6.5% during winter, spring, summer and autumn, respectively. At the same time, there was a slight decrease in soil moisture deficit (< 1.9%) and a slight increase in evapotranspiration (<1.1%) in summer.

If the whole catchment is dominated by grass, the stream flow is expected to decrease slightly in all seasons, 2.6%, 5.2%, 8.4%, and 3.9% during winter, spring, summer and autumn, respectively. The groundwater recharge also slightly decreased by 7.8%, 6.1%, 9.1%, and 5.3% in winter, spring, summer and autumn, respectively. The soil moisture deficit slightly increased by 13.7%, 5.7%, 11.8% and 6.4% and evapotranspiration by 11.3%, 4.7%, 9.7%, and 5.3% in winter, spring, summer and autumn, respectively.

Replacing grass area by oil seed rape, led to a slight decrease (<3%) in stream flow in all seasons apart from autumn where the streamflow was slightly increased by 2.4%. The groundwater recharge also slightly decreased in all season (~2%) apart from autumn, when the recharge increased by 3.9%. Here the soil moisture deficit and evapotranspiration increased slightly by up to 3% and 3.8%, respectively in summer.

Replacing 50% of winter barley with oil seed rape did not produce significant changes to river flow, groundwater recharge, soil moisture deficit and evapotranspiration. The same was observed when 40% of urban area replaced grass and arable area. However, the indication is the urbanization slightly increased (<2%) streamflow and groundwater recharge.

Urban expansion is projected to result in increased streamflow, likely to increase in flood risk. Decreasing the area of the crops like winter barley and grass area and increasing the area of the oil seed rape would result in an increase of soil moisture deficit and a slight decrease in river stream flow, as oil seed rape is expected to take up more water during the spring season when the maximum plant growth takes place. Overall the impact of land use changes on the hydrological variables was less than the effect of climate change. However, land use change is crucial in mitigating the impact of climate change by introducing more sustainable land use practices which could reduce the impact of extreme events, both floods and droughts.

4. Discussion

This study analysed the impact of climate change on the possible occurrence of the drought events and the changes in streamflow and groundwater recharge of the Pang catchment. A number of drought indices were used in the study, which clearly identified all the historic droughts events, i.e. the 1970s, 1980s, 1990s as reported [42]

The application of a wider range of drought indices could be used to identify different types of drought. For example, in agriculture, when soil moisture deficit, *SMD* or Wetness Index, *WI* of the root zone, reach a critical

level, crops will require irrigation, particularly during the summer months which could add more pressure on the water supplies. The *WI* value, if close to 1, would indicate a wet catchment with a possible runoff generation during the next rainfall event. It is a help to reservoir managers to know the *WI* in real time. *RDI* would be helpful for short and long-term planning by water authorities and water companies. Therefore, the findings from the modelling work can be used to review the surface water abstraction regulations based on the successful test of the hydrological model which proved to be a good tool to reproduce the present and past stream flow and to predict future river flow, recharge to groundwater and the other elements of the hydrological cycle.

Considering the possible future increase in water demand for agriculture, a possible solution would be to consider less water consuming crops such as quinoa, amaranth, lucerne and barley. The implication of water abstractions during drought and low flow period would reduce river flows, possibly below the minimum environmental limit. Alternatively, restrictions on abstraction to maintain the minimum environmental flows may restrict crop yields and food or bio- energy crop production. It is important to study groundwater recharge in the Pang catchment as chalk, the main aquifer in the catchment, releases the stored groundwater slowly to the river by base-flow. The effect of low rainfall and high temperature could be expressed by the *RDI* drought index that was able to show more severity and frequency of drought events in the latter half of the century (Figure 9). Considering the possibility of such droughts in the future, the agriculture and irrigation practices need to be adapted for the future as reduced water supply could be problematic for the irrigation in summer. The implication of water abstractions during drought and low flow period would reduce river flows possibly below the minimum environmental limit. Alternatively, restrictions on abstraction to maintain the minimum environmental flows may restrict crop yields and food (or energy) production.

5. Conclusion

The DiCasM model calibration and validation results showed a good agreement between the observed and the simulated flow with high overall model efficiency/goodness of fit. The Nash - Sutcliffe efficiency factor NSE, was above 82% for the 43year's period. In addition to the stream flow, the DiCaSM hydrological model identified all past drought events of the 1970s, the 1980s, 1990s and the most recent ones in 2010-2011, using the drought indices, *SPI*, *RDI*, *SMD*, and the *WI*. Under the UKCP09 climate change projection, the streamflow and the groundwater recharge significantly decreased with time and with emission level specifically during the summer months and the number, frequency and severity of the drought events significantly increased over time and with the increasing the emission level.

Using the joint probability change factors, the stream flow and groundwater recharge are expected to decrease with time and with increasing the emission level by 37% and 70%, in the 2080s during summer and autumn, respectively.

The highest impact of land use change was projected when increasing broad leaf forest. It would reduce stream flow and groundwater recharge by 15% and 19% during spring and summer, respectively. The other changes in land use produced small changes in stream flow and groundwater recharge of less than 10%.

These findings would help in planning for perhaps extra water infrastructure work if needed, such as building more reservoirs or water transfer pipelines from water-rich to water-poor regions, e.g. from Wales to the South East, and adopting a contingency plan for future irrigation water demand. The findings of the study are helpful in managing the abstraction management strategy for the studied Pang catchment and reviewing of existing licensing abstraction limits.

The results of the Pang catchment are applicable to the other catchments of the region and would help in future regional planning and management of the water resources in the southeast of England.

Acknowledgements

The authors acknowledge the NERC funding for this 4-year “Drought Risk and You, DRY” project, grant reference NE/L010292/1. They thank their CEH colleagues, Yan Weigang, Egon Dumont, Virginie Keller and James Blake, who helped preparing the soil model input data and Lindsey McEwen (UWE) who helped organising Local Advisory Group meetings for the Pang catchment. The authors acknowledge the data sources: background mapping from Ordnance Survey (‘1:250 000 Scale Colour Raster’); catchment boundary and gauging station location data from CEH; river and waterbody data from CEH ‘Digital Rivers 50km GB’ Web Map Service; land cover data from CEH Land Cover Map 2007 (25m raster, GB) Web Map Service, Standardized Precipitation Index time series for IHU groups (1961-2012) [SPI_IHU_groups] data licensed from NERC CEH; soils data courtesy of Cranfield University (1:250 000 Soils for England and Wales Web Map Service; Hydrogeology data from British Geological Survey (DiGMapGB 1:625 000 scale digital hydrogeological data.

References

- [1] Wen, Y., Schoups, G., and Van De Giesen, N., Organic pollution of rivers: Combined threats of urbanization, livestock farming and global climate change. *Scientific reports*,7(Article Number 43289). February 2017.
- [2] Griffiths, J., Binley, A., Crook, N., Nutter, J., Young, A., and Fletcher, S., Streamflow generation in the Pang and Lambourn catchments, Berkshire, UK. *Journal of Hydrology*, 330(1-2). 71-83. October 2006.
- [3] Crooks, S., and Kay, A., Simulation of river flow in the Thames over 120 years: evidence of change in rainfall-runoff response? *Journal of Hydrology: Regional Studies*, 4(Part B). 172-195. September 2015.
- [4] Oudin, L., Andréassian, V., Lerat, J., and Michel, C., Has land cover a significant impact on mean annual streamflow? An international assessment using 1508 catchments. *Journal of hydrology*, 357(3-4). 303-316. August 2008.
- [5] Birkinshaw, S.J., Bathurst, J.C., and Robinson, M., 45 years of non-stationary hydrology over a forest plantation growth cycle, Coalburn catchment, Northern England. *Journal of Hydrology*, 519(Part A). 559-573. November 2014.
- [6] Miller, J.D., Kim, H., Kjeldsen, T.R., Packman, J., Grebby, S., and Dearden, R., Assessing the impact of urbanization on storm runoff in a peri-urban catchment using historical change in impervious cover. *Journal of Hydrology*, 515. 59-70. July 2014.
- [7] Parsons, D.J., Rey, D., Tanguy, M., and Holman, I.P., Regional variations in the link between drought indices and reported agricultural impacts of drought. *Agricultural Systems*, 173. 119-129. July 2019.
- [8] Wable, P.S., Jha, M.K., and Shekhar, A., Comparison of Drought Indices in a Semi-Arid River Basin of India. *Water Resour Manage*, 33. 75-102. January 2019.
- [9] Zarei, A.R., Moghimi, M.M., and Bahrami, M. Comparison of reconnaissance drought index (RDI) and effective reconnaissance drought index (eRDI) to evaluate drought severity. *Sustain. Water Resour. Manag.*, 5. 1345-1356. April 2019.
- [10] Ragab, R., and Bromley, J. IHMS—Integrated Hydrological Modelling System. Part 1. Hydrological processes and general structure. *Hydrological processes*, 24(19). 2663-2680. August 2010.
- [11] Montenegro A., and Ragab, R., Hydrological response of a Brazilian semi-arid catchment to different land use and climate change scenarios: a modelling study. *Hydrological Processes*. 24(19). 2705-2723. May 2010.
- [12] Montenegro S., and Ragab, R., Impact of possible climate and land use changes in the semi-arid regions: a case study from North Eastern Brazil. *Journal of Hydrology*. 434-435, 55-68. April 2012.
- [13] D'Agostino, D.R., Trisorio, L.G., Lamaddalena, N., and Ragab, R., Assessing the results of scenarios of climate and land use changes on the hydrology of an Italian catchment: modelling study. *Hydrological processes*, 24(19). 2693-2704. August 2010.
- [14] Ragab, R., Bromley, J., Dörflinger, G., and Katsikides, S., IHMS—Integrated Hydrological Modelling System. Part 2. Application of linked unsaturated, DiCaSM and saturated zone, MODFLOW models on Kouris and Akrotiri catchments in Cyprus. *Hydrological processes*, 24(19). 2681-2692. August 2010.
- [15] Morton, D., Rowland, C., Wood, C., Meek, L., Marston, C., Smith, G., Wadsworth, R., and Simpson, I., Final Report for LCM2007—the new UK land cover map. *Countryside Survey Technical Report*, No 11/07. 2011.
- [16] Morris, D., Flavin, R., and Moore, R., A digital terrain model for hydrology. *4th International Symposium on Spatial Data Handling*, 23-27 July 1990 Zürich. 250-262.
- [17] Morris, D., and Flavin, R., Sub-set of the UK 50 m by 50 m hydrological digital terrain model grids. *NERC, Institute of Hydrology, Wallingford*. 1994.
- [18] NRFA. 2014. *National River flow Archive* [Online]. Available: <http://nrfa.ceh.ac.uk/> [Accessed 2014].
- [19] Allen, R.G., Pereira, L.S., Raes, D., and Smith, M. Crop evapotranspiration-Guidelines for computing crop water requirements-FAO *Irrigation and drainage paper 56*. FAO, Rome, 300, D05109. 1998.
- [20] Environment-Agency, Kennet and Vale of White Horse Catchment Abstraction Licensing Strategy. 2012.
- [21] Aston, A. Rainfall interception by eight small trees. *Journal of hydrology*, 42(3-4). 383-396. July 1979.
- [22] Von Hoyningen-Huene, J., Die Interzeption des Niederschlags in landwirtschaftlichen Pflanzenbeständen, *Arbeitsbericht Deutscher Verband für Wasserwirtschaft und Kulturbau, DVWK*. 1981.
- [23] Gash, J.H., Lloyd, C., and Lachaud, G., Estimating sparse forest rainfall interception with an analytical model. *Journal of Hydrology*, 170(1-4). 79-86. August 1995.
- [24] Raupach, M., Vegetation-atmosphere interaction and surface conductance at leaf, canopy and regional scales. *Agricultural and Forest Meteorology*, 73(3-4). 151-179. March 1995.
- [25] Philip, J., The theory of infiltration: 1. The infiltration equation and its solution. *Soil science*, 83(5), 345-358. May 1957.
- [26] Green, W.H., Studies on soil physics, Part I, the flow of air and water through soils. *J. Agric. Sci.*, 4(1). 1-24. May 1911.
- [27] Ragab, R., Finch, J., and Harding, R., Estimation of groundwater recharge to chalk and sandstone aquifers using simple soil models. *Journal of Hydrology*, 190(1-2). 19-41. March 1997.
- [28] Yu, P.-S., and Jeng, Y.-C., A study on grid based distributed rainfall runoff models. *Water resources management*, 11. 83-99. April 1997.

- [29] Nash, J.E., and Sutcliffe, J.V., River flow forecasting through conceptual models part I—A discussion of principles. *Journal of hydrology*, 10(3). 282-290. April 1970.
- [30] Krause, P., Boyle, D.P., and Bäse, F., Comparison of different efficiency criteria for hydrological model assessment. *Advances in Geosciences*, 5. 89-97. December 2005.
- [31] McKee, T.B., Doesken, N.J., and Kleist, J., The relationship of drought frequency and duration to time scales, In *Proceedings of the 8th Conference on Applied Climatology*, 1993. American Meteorological Society Boston, MA, 179-183.
- [32] Tsakiris, G., Pangalou, D., and Vangelis, H., Regional drought assessment based on the Reconnaissance Drought Index (RDI). *Water resources management*, 21. 821-833. May 2007.
- [33] Vangelis, H., Tigkas, D., and Tsakiris, G., The effect of PET method on Reconnaissance Drought Index (RDI) calculation. *Journal of Arid Environments*, 88. 130-140. January 2013.
- [34] Al-Faraj, F.A., Scholz, M., Tigkas, D., and Boni, M., Drought indices supporting drought management in transboundary watersheds subject to climate alterations. *Water Policy*, 17(5), 865-886. January 2015.
- [35] Khalili, D., farnoud, T., Jamshidi, H., Kamgar-Haghighi, A.A., and Zand-Parsa, S., Comparability analyses of the SPI and RDI meteorological drought indices in different climatic zones. *Water resources management*, 25. 1737-1757. January 2011.
- [36] Narasimhan, B., and Srinivasan, R., Development and evaluation of Soil Moisture Deficit Index (SMDI) and Evapotranspiration Deficit Index (ETDI) for agricultural drought monitoring. *Agricultural and forest meteorology*, 133(1-4). 69-88. November 2005.
- [37] Keshavarz, M.R., Vazifedoust, M., and Alizadeh, A., Drought monitoring using a Soil Wetness Deficit Index (SWDI) derived from MODIS satellite data. *Agricultural Water Management*, 132. 37-45. January 2014.
- [38] Ragab, R., Kaelin, A., Afzal, M. and Panagea, I., Application of Generalized Likelihood Uncertainty Estimation (GLUE) at different temporal scales to reduce the uncertainty level in modelled river flows. *Hydrological Sciences Journal*, Published on line. 65(11). 1856-1871. June 2020.
- [39] Marsh, T., Cole, G., and Wilby, R., Major droughts in England and Wales, 1800-2006. *Weather*, 62(4). 87-93. April 2007.
- [40] Herrera - Pantoja, M., and Hiscock, K., The effects of climate change on potential groundwater recharge in Great Britain. *Hydrological Processes*, 22(1). 73-86. June 2008.
- [41] Alexander, L.V., Tett, S.F., and Jonsson, T., Recent observed changes in severe storms over the United Kingdom and Iceland. *Geophysical Research Letters*, 32(13). 1-4. July 2005.
- [42] Marsh, T., and Monkhouse, R., Drought in the United Kingdom, 1988-92. *Weather*, 48(1). 15-22. January 1993.



© The Author(s) 2020. This article is an open access article distributed under the terms and conditions of the Creative Commons Attribution (CC BY) license (<http://creativecommons.org/licenses/by/4.0/>).